Mathematics and Statistics Department Faculty Publication Series

Mathematics and Statistics

2008

Stability of discrete dark solitons in nonlinear Schrodinger lattices

DE Pelinovsky

PG Kevrekidis
University of Massachusetts - Amherst, kevrekid@math.umass.edu

Stability of Discrete Solitons in the Presence of Parametric Driving

H. Susanto,[1] Q.E. Hoq,[2] and P.G. Kevrekidis[1]

[1]*Department of Mathematics and Statistics, University of Massachusetts, Amherst MA 01003-4515, USA*
[2]*Department of Mathematics, Western New England College, Springfield, MA, 01119, USA*

In this brief report, we consider parametrically driven bright solitons in the vicinity of the anti-continuum limit. We illustrate the mechanism through which these solitons become unstable due to the collision of the phase mode with the continuous spectrum, or eigenvelues bifurcating thereof. We show how this mechanism typically leads to *complete destruction* of the bright solitary wave.

Introduction. In the past few years, differential-difference dispersive equations where the evolution variable is continuum but the spatial variables are discrete, have been the focus of intense research efforts [1]. The key reason for the increasing interest in this research direction can be attributed to the wide range of pertinent applications ranging, from e.g., the spatial dynamics of optical beams in coupled waveguide arrays in nonlinear optics [2], to the temporal evolution of Bose-Einstein condensates (BECs) in deep, optically-induced, lattice potentials in soft-condensed matter physics [3], or even to the DNA double strand in biophysics [4] among others.

One of the key models that has emerged in all of the above settings, either as describing e.g., the envelope wave of the electric field in the optical setting [5], or describing the wavefunction at the nodes of the optical lattice in BECs [6], is the discrete nonlinear Schrödinger (DNLS) equation. This prototypical lattice model features a dispersive coupling between nearest-neighbors, and a cubic onsite nonlinearity.

The above spatially discrete model bears a number of interesting similarities and differences, in comparison with its continuum sibling, the famous (integrable in 1-spatial dimension) nonlinear Schrödinger equation (NLS) [7]. One of the key differences is the breaking of one of the important invariances of the NLS model, namely of the translational invariance that is responsible for momentum conservation in that setting. On the contrary, the discrete model carries an integer-shift invariance. This has some important implications, among other things, to the nature of the solutions of the discrete model. In fact, it was realized through perturbative calculations [8] and subsequently more rigorously justified [9] that the principal (single-humped solitary wave) solutions of the latter model can only be centered on a lattice site or between two lattice sites. In the continuum case, the center of the solution is a free parameter due to the continuum invariance.

On the other hand, one of the important similarities of the discrete model to the continuum one is the presence of the so-called phase or gauge invariance (which is associated with the overall freedom of selecting the solution's phase). The conservation law related to this invariance is the one of the L^2 (respectively l^2) norm, or "mass" of the solution. This invariance is the main focal point of the present work. In particular, we introduce, arguably, the simplest possible perturbation that breaks the rele-

vant invariance, in the form of a parametric drive. The relevance of such a term involving a perturbation proportional to the complex conjugate of the field has been discussed in a variety of earlier works (see e.g. [10] and references therein). A specific physical setting where this type of perturbation arises can be found by looking at the envelope equation of a system of parametrically driven (undamped) coupled torsion pendula as discussed in [11] (with the difference that the envelope wave expansion should be performed in a genuinely discrete setting similarly to [12] rather than near the continuum limit as in [11]). The aim of this exposition is to examine how the breaking of this invariance results in an eigenvalue that bifurcates from the origin of the spectral plane, when linearizing around the most fundamental, solitary wave solution. We argue (analytically and support numerically) that this eigenvalue can lead to an instability of the solitary wave for an isolated value of the parametric drive even at the so-called anti-continuum limit where lattice sites are uncoupled. For non-vanishing couplings, the same eigenvalue leads to a wide interval of parametric instabilities in the two-parameter space (of parametric drive versus inter-site coupling) that we explore both analytically and numerically. Within this interval, we also elucidate the typical numerical behavior of the solitary wave solutions, using direct numerical simulations of relevant unstable waveforms.

Our presentation will be structured as follows. In the next section, we present our analytical setup and perturbative results. Then, we compare our analytical findings with the results of numerical computations. Finally, we summarize our findings and present our conclusions, as well as motivate some questions for future study.

Setup and perturbation analysis. The model we consider is the perturbed (i.e., parametrically driven) discrete non-linear Schrödinger equation of the form

$$i\dot{\phi}_n = -C\Delta_2\phi_n - |\phi_n|^2\phi_n + \Lambda\phi_n + \gamma\overline{\phi_n}, \qquad (1)$$

where C is the coupling constant between two adjacent sites of the lattice, $\Delta_2\phi_n = (\phi_{n+1}-2\phi_n+\phi_{n-1})$ is the discrete Laplacian, Λ is the propagation constant in optics or the chemical potential in BECs, and γ is the strength of the parametric drive.

We focus our attention on a standing wave profile so that ϕ_n is time-independent. In this case, ϕ_n satisfies

$$-C\Delta_2\phi_n - \phi_n^3 + \Lambda\phi_n + \gamma\phi_n = 0. \qquad (2)$$

In the uncoupled (or so-called anti-continuum) limit of $C = 0$, the solution of (2) is $\phi_n = 0, \pm\sqrt{\Lambda + \gamma}$. We examine here the most fundamental single-hump solitary wave solutions which in the anti-continuum limit emanate from a single-site excitation of the form:

$$u_n^0 = 0, \, n \neq 0, \quad u_0^0 = \sqrt{\Lambda + \gamma}. \tag{3}$$

The continuation of (3) for small coupling C can be calculated analytically through a perturbative expansion. By substituting into the steady state equation (2) $u_n = u_n^0 + C u_n^1 + C^2 u_n^2 + \ldots$, one can calculate that up to order $\mathcal{O}(C^2)$

$$u_n = \begin{cases} \sqrt{\Lambda + \gamma} + C/\sqrt{\Lambda + \gamma}, & n = 0, \\ C/\sqrt{\Lambda + \gamma}, & n = -1, 1, \\ 0, & n \, \text{otherwise}. \end{cases} \tag{4}$$

To perform linear stability analysis to the discrete solitary waves of the form of Eq. (4), we introduce the following linearization ansatz

$$\phi_n = u_n + \delta\epsilon_n.$$

Substituting into (1) yields the following linearized equation to $\mathcal{O}(\delta)$

$$i\dot{\epsilon}_n = -C\Delta_2\epsilon_n - 2|u_n|^2\epsilon_n - u_n^2\overline{\epsilon_n} + \Lambda\epsilon_n + \gamma\overline{\epsilon_n}. \tag{5}$$

Writing $\epsilon_n(t) = \eta_n + i\xi_n$ and assuming that u_n is real, eq. (5) gives (see, e.g., [13])

$$\begin{pmatrix} \dot{\eta}_n \\ \dot{\xi}_n \end{pmatrix} = \begin{pmatrix} 0 & \mathcal{L}_+(C) \\ -\mathcal{L}_-(C) & 0 \end{pmatrix} \begin{pmatrix} \eta_n \\ \xi_n \end{pmatrix} = \mathcal{H} \begin{pmatrix} \eta_n \\ \xi_n \end{pmatrix}, \tag{6}$$

where the operator $\mathcal{L}_-(C)$ and $\mathcal{L}_+(C)$ are defined as $\mathcal{L}_-(C) \equiv -C\Delta_2 - (3u_n^2 - \Lambda - \gamma)$ and $\mathcal{L}_+(C) \equiv -C\Delta_2 - (u_n^2 - \Lambda + \gamma)$. The stability of u_n is then determined by the eigenvalues of $\mathcal{H}$.

Let the eigenvalues of $\mathcal{H}$ be denoted by $i\omega$, which implies that u_n is stable if $\text{Im}(\omega) = 0$. Because (6) is linear, we can eliminate one of the 'eigenvectors', for instance ξ_n, from which we obtain the following eigenvalue problem

$$\mathcal{L}_+(C)\mathcal{L}_-(C)\eta_n = \omega^2\eta_n = \Omega\eta_n. \tag{7}$$

As before, we expand the eigenvector η_n and the eigenvalue Ω as

$$\eta_n = \eta_n^0 + C\eta_n^1 + \mathcal{O}(C^2), \quad \Omega = \Omega^0 + C\Omega^1 + \mathcal{O}(C^2).$$

Substituting into Eq. (7) and identifying coefficients for consecutive powers of the small parameter C yields

$$\left[\mathcal{L}_+(0)\mathcal{L}_-(0) - \Omega^0\right]\eta_n^0 = 0, \tag{8}$$

$$\left[\mathcal{L}_+(0)\mathcal{L}_-(0) - \Omega^0\right]\eta_n^1 = f, \tag{9}$$

with

$$f = \left[-(\Delta_2 + 2u_n^0 u_n^1)\mathcal{L}_-(0) - \mathcal{L}_+(0)(\Delta_2 + 6u_n^0 u_n^1) + \Omega^1\right]\eta_n^0. \tag{10}$$
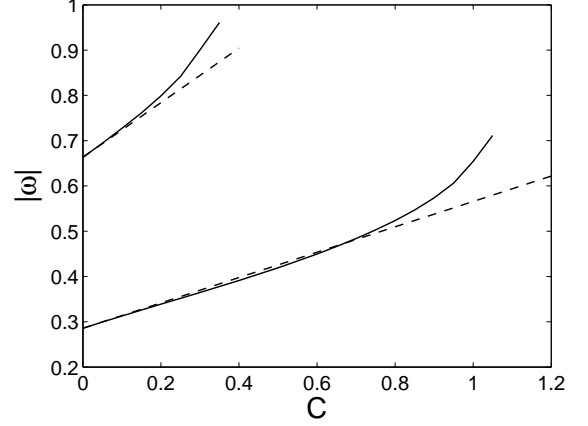

FIG. 1: The smallest eigenvalue for two values of γ, namely $\gamma = 0.02$ and $\gamma = 0.1$. The dashed lines are the approximate analytical estimate of the relevant frequency from Eq. (12). The lower curves correspond to $\gamma = 0.02$.

First, let us consider the order $\mathcal{O}(1)$ equation (8). One can do a simple analysis to show that there are only two eigenvalues, i.e., $\Omega^0 = \Lambda^2 - \gamma^2$ and $\Omega^0 = 4(\Lambda + \gamma)\gamma$. $\Omega^0 = \Lambda^2 - \gamma^2$ has infinite multiplicity and is related to the continuous spectrum that will be discussed later. Therefore, our interest is in $\Omega^0 = 4(\Lambda + \gamma)\gamma$ that has the normalized eigenvector $\eta_n^0 = 0, \, n \neq 0$ and $\eta_0^0 = 1$. This eigenvalue is the formerly zero eigenvalue due to the phase or gauge invariance of the DNLS equation *in the absence of parametric driving*.

The continuation of the eigenvalue $\Omega^0 = 4(\Lambda + \gamma)\gamma$ when the coupling C is turned on can be calculated from Eq. (9). Due to the corresponding eigenvector having $\eta_n^0 = 0$ for $n \neq 0$, we only need to consider the site $n = 0$. In this case, $f = -8\gamma + \Omega^1$. The solvability condition of Eq. (9) using, e.g., the Fredholm alternative requires $f = 0$ from which we immeadiately obtain that $\Omega^1 = 8\gamma$. Hence, the smallest eigenvalue of a one-site discrete soliton solution of Eq. (1) is

$$\Omega = 4(\Lambda + \gamma)\gamma + 8\gamma C + \mathcal{O}(C^2), \tag{11}$$

or

$$\omega = \pm 2\sqrt{(\Lambda + \gamma)\gamma} \pm 2\frac{\gamma}{\sqrt{(\Lambda + \gamma)\gamma}}C + \mathcal{O}(C^2). \tag{12}$$

If $\gamma = \mathcal{O}(C)$, Eq. (12) becomes

$$\omega = \pm 2\sqrt{\Lambda\gamma}\sqrt{C} + \mathcal{O}(C). \tag{13}$$

Next, we have to proceed with calculating the continuous spectrum of the operator $\mathcal{L}_+(C)\mathcal{L}_-(C)$ (7). When $C = 0$, all the continuous spectrum of the operator lies at $\Omega = \Lambda^2 - \gamma^2$ as was mentioned before. When C is increased, the eigenvalues spread on the imaginary axis creating a phonon band. Using a plane wave expansion $\eta_n = ae^{i\kappa n} + be^{-i\kappa n}$ yields the dispersion relation

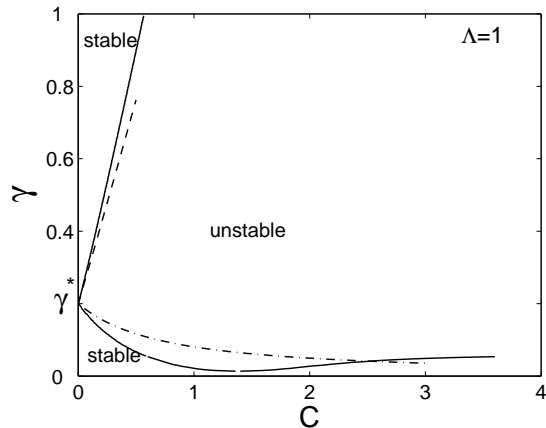$$\Omega = (\Lambda + \gamma + 2C - 2C\cos\kappa)(\Lambda - \gamma + 2C - 2C\cos\kappa).$$

FIG. 2: The stability-instability region in the two-parameter space $\gamma - C$. The solid lines give the numerically obtained separatrices, while the dash-dotted and dashed ones the analytical approximations of Eqs. (14) and (15) respectively.
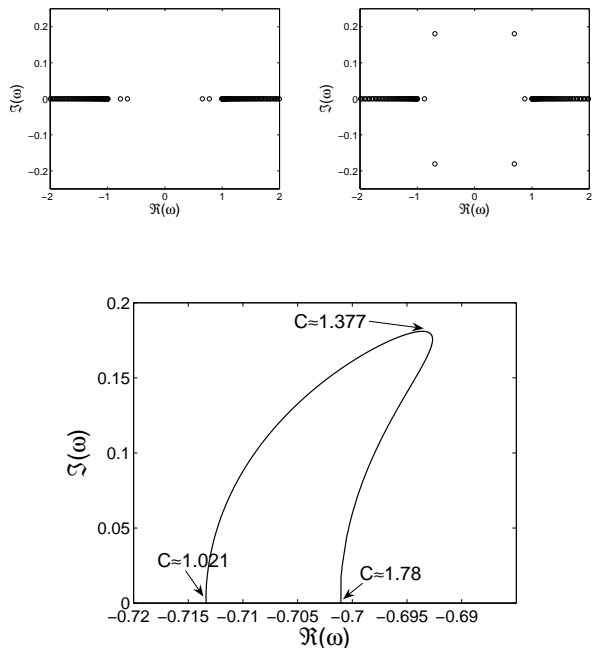

FIG. 3: The eigenvalue structure of a single-hump solitary wave for $\gamma = 0.02$ and $C = 1.0$ (top left panel), as well as $C = 1.4$ (top right panel). The bottom panel shows the trajectory of one of the unstable eigenvalues as C changes.

Hence, the continuous band lies between $\Omega_L = \Lambda^2 - \gamma^2$ (when $\kappa = 0$) and $\Omega_U = \Lambda^2 - \gamma^2 + 8C(\Lambda + 2C)$ (when $\kappa = \pi$).

For small γ, the instability of a one-site discrete breather of (1) is caused by the collision of the smallest eigenvalue (11) with an eigenvalue bifurcating from Ω_L. However, here we assume that the bifurcating eigenvalue does not move very fast in the spectral plane such
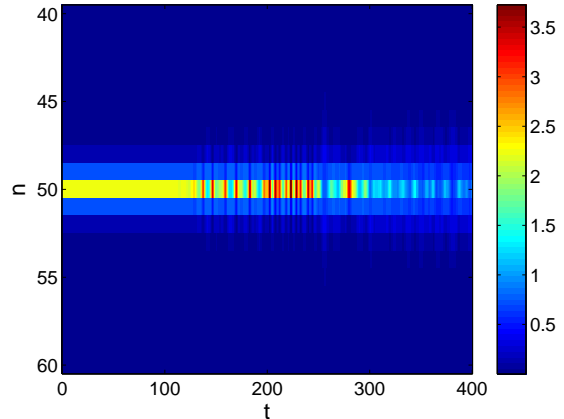

FIG. 4: (Color online) The spatio-temporal evolution of an unstable single-hump solitary wave at $\gamma = 0.02$ and $C = 1.4$. The contour plot of square modulus $|\phi_n|^2$ is shown.

that it can be represented by Ω_L. For large γ, the instability is due to the collision of the smallest eigenvalue and Ω_L. Equating those quantities will give the critical γ as a function of the coupling constant C, i.e.

$$\gamma_{\mathrm{cr}}^1 = -\frac{2}{5}\Lambda - \frac{4}{5}C + \frac{1}{5}\sqrt{9\Lambda^2 + 16C(\Lambda + C)}, \quad (14)$$

$$\gamma_{\mathrm{cr}}^2 = -\frac{2}{5}\Lambda - \frac{4}{5}C + \frac{1}{5}\sqrt{9\Lambda^2 + 56C\Lambda + 96C^2}. \quad (15)$$

The two approximate γ_{cr}^i above coincide at $C = 0$ and $\gamma^* = (\sqrt{2} - 1)/2 \approx 0.2071$. Notice that at that level the relevant calculation is analytically exact (i.e., there is no approximation and the solitary excitation will be unstable for $C = 0$ only for $\gamma = \gamma^*$).

Numerical results. We now proceed to testing our analytical results for the parametrically driven discrete nonlinear Schrödinger system numerically. We start by examining the validity of our analytical prediction for the eigenfrequency corresponding to the phase mode which bifurcates from $\omega = 0$ because of the presence of the parametric drive according to the expression (12). Figure 1 shows this prediction as a function of C for two different values of γ. Clearly the prediction is fairly accurate for small C and its range of validity is wider for smaller values of γ.

We now turn to the examination of the two parameter-plane of the parametric drive γ versus the coupling strength C. Figure 2 provides a full description of the dynamics of the parametrically driven DNLS model regarding the intervals of stability/instability of the most fundamental, single-hump solitary wave solution of the model. The solid lines show the numerically obtained separatrices between the stable and unstable parametric regimes of the model, while the dashed and dash-dotted lines give the analytical prediction for the stability range as obtained by the conditions of collision of the phase mode eigenfrequency with the continuous spectrum from

Eqs. (14)-(15). We observe that the prediction of Eq. (15) is in very good agreement with the numerical observations for the occurrence of the instability point. This is because the collision typically occurs indeed with the upper band edge of the continuous spectrum (rather than with an eigenvalue bifurcating from it) and also typically the collision occurs for small C for which the analytical approximation of Eq. (12) is a very good approximation. On the other hand, the slightly less satisfactory agreement with the prediction of Eq. (14) occurs due to the collision with eigenvalues bifurcating from the lower edge of the continuous spectrum (see also Fig. 3 below) and also for relatively large C's for which higher order terms in the expansion of (12) should be expected to contribute.

Figure 3 illustrates the typical instability scenario for weak parametric drives ($\gamma = 0.02$ in this figure). As C increases, the eigenvalue which is associated with the phase mode moves towards the continuous spectrum (top left panel). Eventually for $C \approx 1.021$ it collides with an eigenvalue pair that has bifurcated from the lower band edge of the continuous spectrum. Due to the opposite Krein signature of these eigenvalues (see e.g. the relevant discussion in [14]), their collision leads to an oscillatory instability and the bifurcation of a complex quartet of eigenvalues (top right panel). Eventually, as is shown in the bottom panel, the eigenfrequencies return to the real axis to re-stabilize the configuration for $C > 1.78$.

One can also notice from Fig. 2 that there is a minimum γ_m below which the soliton is stable all the way to the continuum limit. Numerically, $\gamma_m \approx 0.0135$. When γ is less than γ_m the eigenvalue (11) that moves towards the continuous spectrum does not collide with the eigenvalue bifurcating from the phonon band Ω_L. Instead, it decreases before the collision occurs. This shows that the second order correction $\mathcal{O}(C^2)$ of (11) dominates the leading order expression.

We now turn to the examination of the dynamical behavior of the unstable solutions obtained above. The direct numerical evolution of an unstable solution of Eq. (1) is shown in Figure 4. We have confirmed that this dynamics is typical of the unstable parameter range. The figure shows that eventually the solution becomes subject to the oscillatory instability that was illustrated in Fig. 3 and is ultimately destroyed completely. This may also be expected on the basis of the fact that this is the fundamental coherent structure solution and for the same parameter set there appears to be no other stable dynamical state (other than $\phi_n = 0$) to which the initial condition may transform.

Conclusions. In this short communication, we visited the topic of parametrically driven lattices of the nonlinear Schrödinger type. We have shown that the dynamics of these lattices is considerably different than those of the regular DNLS equation. This is due to the driving-induced bifurcation of the phase mode (associated with the gauge invariance of the NLS equation). Collision of this mode with eigenfrequencies stemming from the continuous spectrum leads to a wide parametric regime of instabilities of the fundamental solitary wave in this model. Our perturbative analysis captures quite accurately the relevant eigenvalue (especially for weak couplings) and provides a fair estimate of the instability threshold in the parameter-space of the system. The result of the ensuing oscillatory instability is the destruction of the fundamental soliton, a feature absent from the regular DNLS model (where this solution is stable for all parameter values).

It would be interesting to expand the present considerations to other variants of the discrete parametrically driven model such as its higher-dimensional analogs, the defocusing case, or also damped variants of these lattice models. Such considerations are currently under study and will be reported in future publications.

[1] S. Aubry, Physica D **103**, 201, (1997); S. Flach and C.R. Willis, Phys. Rep. **295** 181 (1998); D. Hennig and G. Tsironis, Phys. Rep. **307**, 333 (1999); P.G. Kevrekidis, K.O. Rasmussen, and A.R. Bishop, Int. J. Mod. Phys. B **15**, 2833 (2001).

[2] D. N. Christodoulides, F. Lederer and Y. Silberberg, Nature **424**, 817 (2003); Yu. S. Kivshar and G. P. Agrawal, *Optical Solitons: From Fibers to Photonic Crystals*, Academic Press (San Diego, 2003).

[3] P.G. Kevrekidis and D.J. Frantzeskakis, Mod. Phys. Lett. B **18**, 173 (2004). V.V. Konotop and V.A. Brazhnyi, Mod. Phys. Lett. B **18** 627, (2004); P.G. Kevrekidis *et al.*, Mod. Phys. Lett. B **18**, 1481 (2004).

[4] M. Peyrard, Nonlinearity **17**, R1 (2004).

[5] D.N. Christodoulides and R.I. Joseph, Opt. Lett. **13**, 794 (1988).

[6] A. Trombettoni and A. Smerzi, Phys. Rev. Lett. **86**, 2353 (2001).

[7] C. Sulem and P.L. Sulem, *The Nonlinear Schrödinger Equation*, Springer-Verlag (New York, 1999).

[8] Yu.S. Kivshar and D.K. Campbell, Phys. Rev. E **48**, 3077 (1993).

[9] T. Kapitula and P. Kevrekidis, Nonlinearity **14**, 533 (2001).

[10] N.V. Alexeeva, I.V. Barashenkov and D.E. Pelinovsky, Nonlinearity **12**, 103 (1999); I.V. Barashenkov and E.V. Zemlyanaya, Phys. Rev. Lett. **83**, 2568 (1999) I.V. Barashenkov, S.R. Woodford and E.V. Zemlyanaya, Phys. Rev. Lett. **90**, 054103 (2003).

[11] N.V. Alexeeva, I.V. Barashenkov and G.P. Tsironis Phys. Rev. Lett. **84**, 3053 (2000).

[12] Yu.S. Kivshar and M. Peyrard, Phys. Rev. A **46**, 3198 (1992).

[13] M. Johansson and Yu. S. Kivshar, Phys. Rev. Lett. **82**, 85-88 (1999).

[14] T. Kapitula, P.G. Kevrekidis and B. Sandstede, Physica D **195**, 263 (2004).